This paper is available online at www.praiseworthyprize.org
International Journal on Communications Antenna and Propagation (I.Re.C.A.P.), Vol. 13, N. 1
ISSN 2039 – 5086 February 2023

Design and Implementation of a 2.4-GHz Fully Integrated Butler Matrix for Smart Antenna System

S. Montoya-Villada[1], J. Morales-Guerra[1], D. Cataño-Ochoa[1], J. Zapata-Londoño[1], J. Botero-Valencia[2], Erick Reyes-Vera[1]

Abstract – *This work proposes and analyzes a low-cost fixed microstrip beamforming system based on a uniform linear array with four rectangular patch antennas controlled by a Butler matrix that operates in the 2.4 GHz ISM band. A 4×4 Butler matrix consisting of four hybrid quadrature directional couplers, two crossovers, and two 45° phase shifters was designed and implemented to control the beam direction of the entire system. Similarly, a comparative study is performed between two different antenna arrays, the first consisting of a conventional linear antenna array and the second antenna array consisting of four patch antennas loaded with metamaterial structures on the ground plane. Finally, the electrical performance of both smart beamforming systems was evaluated, and their potential application as a wireless power transmitter was evaluated. Four beams with distinct orientations were created in each situation. The smart antenna based on a conventional array has a higher gain, while the smart antenna based on metamaterial structures has a higher HPBW.*

Keywords: *Butler Matrix, Antenna Array, Beamforming, Uniform Linear Array*

Nomenclature

Z_0	Characteristic Impedance [Ω]
tan δ	Loss tangent
ε_r	Relative Dielectric Permittivity
θ	Polar angle [°]
λ	Wavelength [μm]
S_{11}	Return Loss [dB]
HPBW	Half-Power Beamwidth [°]
CSRR	Complementary Split Ring Resonator
ULA	Uniform Linear Array
IoT	Internet of Things
WSN	Wireless Sensor Networks

I. Introduction

The increased interest in Internet of Things (IoT) applications, as well as the expansion of Wireless Sensor Networks (WSNs), has created a need to improve the antennas that are currently utilized to transfer data wirelessly [1]-[4]. In fact, wireless communication systems are often subject to large disturbances that affect the transmission of information, such as environmental changes, channel interference phenomena, and multipath fading. The development of smart antennas with programmable electrical characteristics that can be and are tuned to the particular demands of a connection is an intriguing solution to these issues [5]-[10]. Furthermore, this kind of antenna allows for the concentration of radiation in a specific direction, communication with several users on a single channel, and modification of traffic conditions during operation [10]-[15]. Smart antennas are made up of an array of antennas that may be controlled via various techniques. There are two kinds of smart antenna systems: switched beam systems and adaptive array systems. However, switching beam antennas are simpler and less expensive than adaptive antennas. A switched beam system is made up of a fixed beamforming network, an antenna array, and a Radio Frequency (RF) switch. In this case, the array's radiation pattern is dynamically controlled, and it can generate multiple beams that can be used as a fixed beamforming system [7], [10]. The Rotman lens, Mixer matrix, Nolen matrix, Blas matrix, and Butler matrix are some of the most widely used ways for constructing analog free space communication networks. However, the Butler matrix is the most used method since it is a simple solution that is less costly, has fewer components, and can produce highly focused beams [10], [15]. The Butler matrix is well-known for creating differential phase changes at an antenna array's input using only passive components like as phase shifters, directional couplers, and crossovers [16]. This method has been studied in several recent reports to develop a fixed beamforming system. For example, Abhinav Shastrakar et al. designed and implemented a Butler matrix that operates at ISM band in 2016 [16]. The acquired results show a good correspondence between theoretical and experimental findings. The hybrid coupler has a return loss of -3.363 dB and -3.534 dB for ports 2 and 3, respectively. A

Available online by February 28th, 2023 https://doi.org/10.15866/irecap.v13i1.22234

crossover based on two cascaded hybrid couplers was built, with a -0.805 dB loss in port 3. Finally, a phase shifter of 45° was implemented to complete the Butler matrix. In a similar way, Cabrera et al., proposed and analyzed an antenna with a tunable radiation pattern, which was fed through a Butler matrix [17]. The novelty of this work was that the authors added Wilkinson power dividers to convert the 4×4 matrix into a 4×6 matrix. As a result, the authors reported an antenna with a bandwidth of 415 MHz. On the other hand, due to their peculiar electromagnetic properties, such as negative permittivity and permeability, metamaterial structures have attracted the curiosity of researchers throughout the last two decades [18]-[21], [30]-[33]. In fact, the radiation pattern or the gain of antennas can be manipulated by incorporating metamaterial cells in the vicinity of the radiating part or etched into the substrate [22]-[24]. For example, Dadgarpour et al. inserted an array of *H*-shape unit cells into the bow-tie antenna substrate for tilting the radiation angle [25]. The obtained findings show that it is feasible to deflect the angle while increasing the gain. Esmail et al. presented a similar approach in 2019 [26]. In such instance, the authors use a novel Adjacent Square-Shaped Resonator (ASSR) structure to accomplish beam tilting in a dipole antenna at 3.5 GHz. The research shows that the radiation beam of the dipole antenna is tilted by +25° and 24° depending on how the ASSR array is positioned on the dipole antenna substrate. Dadgarpour et al. (2018) presented an antenna based on three double-sided bowtie radiators loaded by 2×6 Double Split Rectangular (DSR) unit cells, which are arranged vertically on the antenna substrate to produce beam deflection angles of 17° and 20° at the 3.5 and 5.5 GHz bands, respectively [27].

Thus, the incorporation of metamaterials could help to improve the electrical performance of beamforming systems. This work presented a 2.4 GHz microstrip fixed beamforming system based on a uniform linear matrix and four rectangular patch antennas. The proposed structure is unique in that it makes use of an arrangement of metamaterials etched in the ground plane to investigate the effect of this type of element on the electrical characteristics of the proposed fixed beamforming system. A Butler matrix based on phase shifters, directional couplers, and crossover is used to control the radiation pattern. The findings show that this technique is adequate for building a smart antenna and control de radiation pattern direction.

Section II will go through the suggested Butler matrix and antenna designs in further detail. Section III will next go through the Butler matrix simulation findings and the reaction of the fixed beamforming system. Finally, the work's conclusions will be presented.

II. Methodology

This section discusses the fixed beamforming components. The design of each Butler matrix part is presented and illustrated. Afterward, the patch antenna design loaded with metamaterial structures is explained.

II.1. Butler Matrix Design

Butler matrix is a MIMO (Multiple Input, Multiple Output) system of *n* inputs and *n* outputs [15], [29]. It is used as a fixed beam former network of a Uniform Linear Array (ULA) of *n* elements, where *n* is even and is of special interest when *n* is equal to or greater than two; this configuration enables the possibility of steering the beam generated from *n* sub-beams with different directions and is usually called a switched beam system [28]. This study proposes and optimizes a MIMO system composed of four 3-dB hybrid couplers, two 0-dB crossovers, and two 45° phase shifters for operation at 2.4 GHz. This fixed beamformer is used to feed a ULA based on four microstrip patch antennas with inset feed.

In fact, the performance of a conventional linear antenna array and a linear antenna array with metamaterials etched in the ground plane are compared. To create this completely switched beam system, a FR4 substrate with a relative permittivity of 4.3, a loss tangent (tan δ) of 0.0025, a thickness of 1.6 mm, and a copper layer of 35 μm was used. Moreover, the bottom layer is a continuous sheet of copper and the characteristic input impedance (Z_0) of the proposed antenna is set at 50-Ω. Each of these elements will be detailed in the next subsections.

CST Microwave Studio, a program based on the conventional Finite-Difference Time-Domain (FDTD) approach, was used to develop the proposed Butler array.

This program was used to investigate the electromagnetic properties of each component of the Butler array before assembling them to create a fixed beamforming system. Figures 1-4 show each component that was used.

II.2. 90° Hybrid Coupler

Figure 1 shows the schematic of the 90° hybrid coupler. This coupler is based on a passive branch-line, which is characterized because the input power (injected by port 1) is eventually split between ports 2 (through the arm) and port 3 (coupled arm). Similarly, this configuration is frequently used to create a 90° phase shift between ports 2 and 3, while port 4 is isolated. In the proposed design, two pairs of quarter wavelength microstrip lines were employed, with impedances of 50-Ω and 35.35-Ω per pair. The main geometrical parameters of the proposed hybrid coupler are summarized in Table I.

TABLE I
GEOMETRICAL PARAMETERS OF PROPOSED HYBRID COUPLER

Parameter	Value
W	3 mm
W_{h1}	3 mm
W_{h2}	3.72 mm
W_{h3}	5.25 mm
l_{h1}	17.5 mm
l_{h2}	14.15 mm

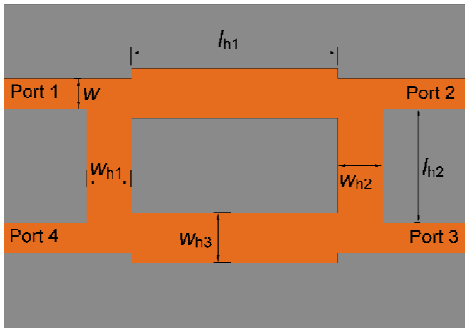

Fig. 1. Schematic of the proposed -3-dB Hybrid coupler

II.3. Crossover (0-dB) Coupler

The 0-dB crossover is shown in Figure 2. It was created by connecting two passive branch-line couplers in series. This kind of microwave circuit works by routing the incoming signal at port 1 to output 3, whereas the signal entering port 4 is sent directly to port 2.

Similarly, this component is an important feature of the Butler matrix since it is an effective way of crossing two transmission lines while reducing coupling between them. Table II defines the geometrical specifications of this component.

II.4. Phase Shifter

A pair of 45° phase shifters has been added to the proposed Butler matrix to ensure the phase difference between all output ports and to compensate for the accumulated losses in the whole matrix. The design of this microstrip component is shown in Figure 3. It should be noted that the geometrical parameters of these phase shifters were varied until the phase difference between the Butler matrix's output ports achieved the desired results.

TABLE II
GEOMETRICAL PARAMETERS OF PROPOSED CROSSOVER COUPLER

Parameter	Value
W_{c1}	3 mm
W_{c2}	6 mm
W_{c3}	5.25 mm
W_{c4}	3 mm
l_{c1}	35.2 mm
l_{c2}	14.15 mm

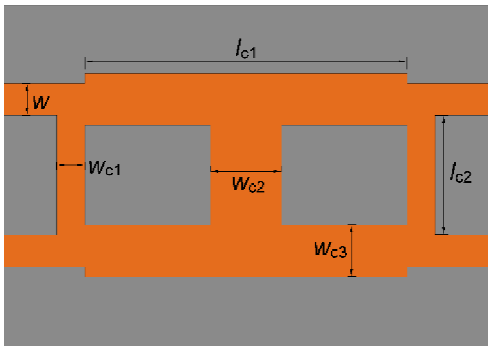

Fig. 2. Schematic of 0-dB crossover

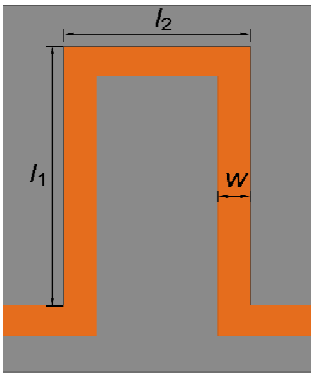

Fig. 3. Schematic of phase shifter

The parameter l_1 and l_2 are equal to 30.42 mm and 20.15 mm respectively, whereas W is the width of the transmission lines connecting the different elements (Table I).

II.5. Microstrip Antenna Design

The second stage of the fixed beamforming system was the integration of the ULA with the Butler matrix.

As previously stated, we investigated and compared the performance of the fixed beamforming system when the Butler array is used in combination with a conventional ULA and a linear antenna array integrating metamaterials etched in the ground plane. Figures 4 depict a microstrip antenna configuration with Complementary Split Ring Resonators (CSRR) in the ground plane.

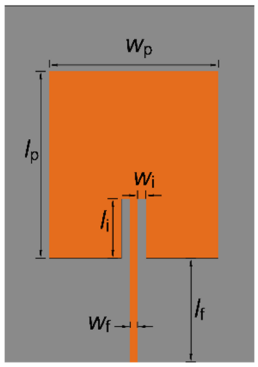

(a)

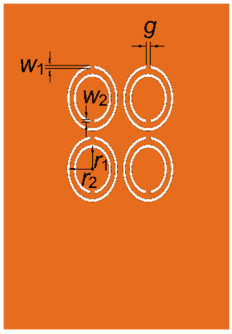

(b)

Figs. 4. Schematic of the proposed patch antenna. (a) present the top view of the patch antenna, (b) shows the bottom view

The conventional ULA design is not displayed since it is identical; the main difference is that the conventional one does not have resonators etched in the ground plane.

Figures 4(a) and 4(b) depict the proposed antenna's top and bottom perspectives, respectively. The suggested patch antenna has 41 mm of width (W_p) and a length (l_p) of 33.9 mm set to operate with the butler matrix at 2.4 GHz; to reduce the losses in the path to the antenna, the feed line was transformed to an impedance of $Z_0\sqrt{2} = 70.7\Omega$.

In addition, to improve the return loss at the antenna's edge, an inset fed coupler formed of two stubs was utilized on both sides of the patch-feed interface. As a result, the ideal impedance is achieved between the antenna's borders and center. Figure 4(b) depicts an arrangement of four double resonator rings etched in the ground plane. The entire geometrical parameters of the proposed antenna and resonator dimensions are summarized in Table III. Finally, a schematic of the proposed fixed beamformer is illustrated in Figure 5.

III. Results and Discussion

In this section, the phase differences of the output ports with their respective radiation pattern will be displayed after unifying the components of the 4×4 butler matrix. For this reason, the implementation of a conventional patch antenna operating at 2.4 GHz in the butler matrix will be analyzed and the basic characteristics of the antenna transmission (Gain, main lobe direction, efficiency, and HPBW) will be examined.

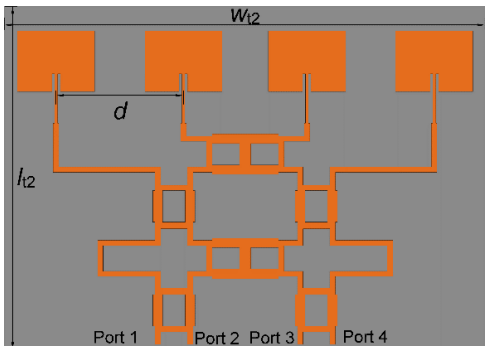

Fig. 5. Schematic of the proposed fixed beamformer

TABLE III
GEOMETRICAL PARAMETERS OF PROPOSED MICROSTRIP ANTENNA

Parameter	Value
w_p	41 mm
l_p	33.9 mm
w_f	1.6 mm
l_f	17.5 mm
w_i	1.4 mm
l_i	10 mm
r_1	6.5 mm
r_2	3.8 mm
w_1	1 mm
w_2	1 mm
g	1 mm
L_{T2}	122.7 mm
W_{T2}	255 mm
d	λ/2

Likewise, the performance of this antenna is compared with the novel structure based on the use of metamaterial arrays etched in the ground plane.

III.1. Butler Matrix Phase Analysis

To begin, each Butler matrix element was examined independently to guarantee minimal losses and good performance at 2.4 GHz. Following that, all components were integrated on the same board, as depicted in Figure 5. Then, the proposed structure was developed further to increase the phase difference between the four output ports (port 5, port 6, port 7, and port 8). The suggested Butler array is then examined with each input port independently connected to an RF input signal. Electromagnetic research was carried out between 2 and 3 GHz. Figure 6(a) depicts the signal phase at port 1's input.

The results reveal a typical behavior on the phase response at the four output ports since the phase at each output is different and the phase response presents a frequency shift in all cases. For example, the phases at 2.4 GHz are -116.70°, -158.15°, 160.59°, and 109.02° for the output ports 5, 6, 7 and 8 respectively. Based on these data, the phase difference between the output ports was estimated.

Thus, the obtained phases differences between the ports 5-6, 7-6, and 8-7 are 41.45°, 41.26°, and 51.57° respectively. Then, the average of this phase difference is 44.76°, which is the expected for the Butler matrix to work properly. When the RF signal arrived through ports 2, 3, and 4, the same analysis was performed. Figures 6(b), 6(c), and 6(d) depict the phase difference, respectively. Table IV further highlights the most relevant findings from the four case studies. The results shown in Figures 6 verify the correct operation of this device since the phase difference between the output ports (5-6, 7-6, and 8-7) operates as expected in literature reports [4], [5]. When the signal is entered through port 1, the goal is to achieve an average phase difference of 45°, and the proposed solution achieves an average phase difference of 44.76°. As a result, the obtained inaccuracy is only 0.53%. Similarly, when the signal comes through ports 2, 3, and 4, the predicted average phase difference is 135°, 135°, and 45°, respectively. The collected data show an average phase difference of 134.28°, 134.42°, and 44.96°.

Table V shows that the average error is less than 1% in all scenarios. These findings show that the suggested Butler matrix functions very near to optimally. As a result, this arrangement is appropriate for use in the design of a fixed beamforming system.

TABLE IV
PHASE DIFFERENCE IN OUTPUT PORTS
WHEN THE RE SIGNAL IS INPUT USING PORTS 1-4

Parameter/Input	Phase 6-5 (°)	Phase 7-6 (°)	Phase 8-7 (°)	Average (°)
Port 1	41.45	41.26	51.57	44.76
Port 2	127.64	135.51	139.69	134.28
Port 3	140.34	134.69	128.24	134.42
Port 4	51.29	42.53	41.08	44.96

TABLE V
ERROR ACQUIRED IN THE DIFFERENCE OF PHASES WITH RESPECT TO AN IDEAL MODEL

Parameter/Input	Error 6-5 (%)	Error 7-6 (%)	Error 8-7 (%)	Average (%)
Port 1	7.88	8.31	14.6	0.53
Port 2	5.45	0.38	3.47	0.53
Port 3	3.95	0.23	5	0.43
Port 4	13.97	5.48	8.71	0.08

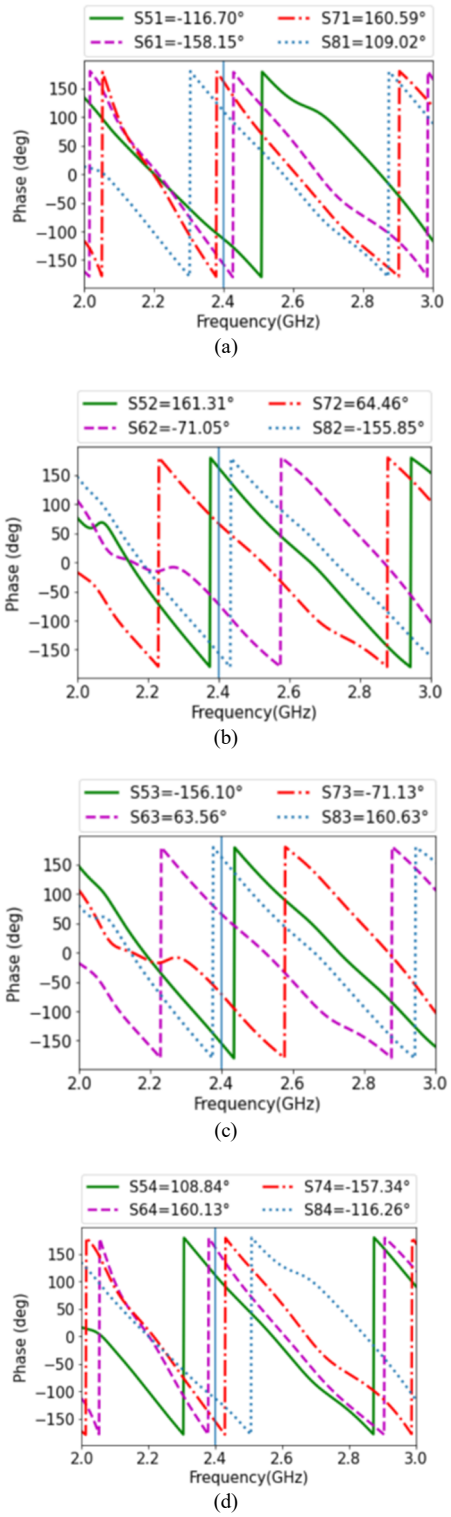

Figs. 6. Phase difference analysis when the RF signal input trough (a) port 1 (b) port 2 (c) port 3 (d) port 4

III.2. Radiation Pattern Antenna Analysis

After confirming that the suggested Butler matrix functioned optimally, either regular ULAs or ULAs with metamaterial structures etched in the ground plane were coupled to it. In both cases the ULA is based on four identical microstrip antennas and it was designed to operate at 2.4 GHz as well, and to be integrated into the same board as the Butler network. The smart antenna (Butler matrix + ULA) has a total width (W_{T2}) of 241.5 mm and a total length (L_{T2}) of 166.55 mm. In addition, to maximize power transfer from the Butler matrix to the ULA, an impedance matching method was implemented. In this case, an inset feed connection was chosen since it is simple and does not require any additional equipment.

A schematic of the whole system of our smart antenna was previously depicted in Figure 5. Finally, the radiation pattern of the smart antenna system was investigated. Thus, the behavior of the proposed fixed beamforming was simulated using CST STUDIO, and experimentally validated in the Laboratory. A RF Generator (Rhode &Schwartz, SMBV-B103) was used to inject the RF signal, and power measurements were collected with a Vector Network Analyzer (Rhode & Schwartz, FSH8). The data were recorded when the antenna was rotated every 5° in phi-plane. The smart antenna system's ability to concentrate radiation in four separate directions was validated in this experiment.

Therefore, the entire system was examined using the two separate ULA options. First, the electrical performance of a smart antenna based on conventional ULA was studied. Figures 7 depict a comparison of the simulated and experimental radiation patterns. Figure 7(a) depicts the whole system's normalized radiation pattern when the signal is entered through port 1. This radiation pattern shows that the major lobe points in a positive degree direction since the phase shift of port 1 is positive, as previously demonstrated (Table IV). In this scenario, the radiation pattern provides energy at 30.0°.

In addition, the obtained gain was -34.7 dB, and the Half-Power Beamwidth (HPBW) was 20°. Similarly, when the signal was entered through ports 2, 3, and 4, the electrical properties of this device were analyzed. The radiation patterns are illustrated in Figures 7(b), 7(c), and 7(d) respectively. From the findings it is easy to note that the direction of the primary lobe varies substantially in all situations, in fact 30°, -35.0°, 49° and -60° are attained, while the achieved gain in these ports were -23.6 dB, -24.03 dB and -32.74 dB respectively. These results demonstrated the suggested smart antenna's ability to control radiation patterns and transfer electromagnetic energy in four distinct directions. In addition, the other electrical characteristics of the smart antenna system were determined. Table VI summarizes the findings. This table indicates that when the signal is entered by ports 1 and 4, the proposed antenna setup has a higher gain. As a result, they might be utilized to establish contact with more distant nodes. Similarly, the HPBW in all situations is extremely comparable and less than 28.0°.

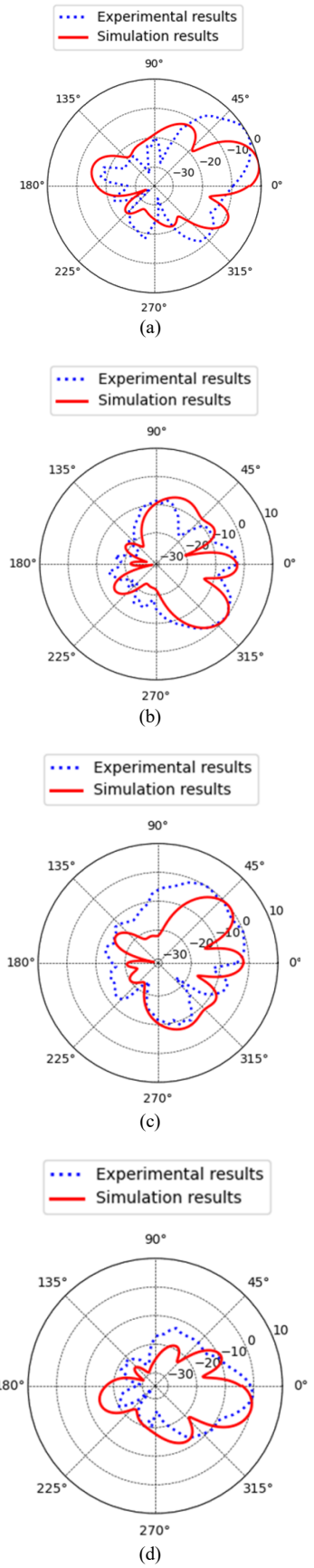

Figs. 7. Comparison between simulated and experimental radiation patterns of the beamforming system based on conventional ULA when the RF signal input trough (a) port 1 (b) port 2 (c) port 3 (d) port 4

TABLE VI
EXPERIMENTAL RADIATION PATTERN OF CONVENTIONAL ULA

Parameter/Input	Port 1	Port 2	Port 3	Port 4
Gain (dbi)	-35.8	-23.7	-22.8	-37.9
Main lobe direction (deg)	15	-35	40	-15
HPBW (deg)	20	25	27	25

Therefore, this system is suited for a wide range of applications where control of the radiation pattern and major lobe direction of transmission is critical, such as indoor positioning, wireless power transfer, wireless sensor networks, and so on. The same parameters were simulated and evaluated using CST STUDIO, and the summary findings are shown in Table VII. To compare theoretical and experimental results in the same condition, the simulated radiation pattern was also obtained each 5° and the gain level was normalized.

From simulation results, the radiation efficiency was obtained when the signal is injected through the different ports.

Thus, the obtained radiation efficiency was -0.4630 dB (89.88%), 0.6615 dB (85.87%), 0.6829 dB (85.44%), and 0.4534 dB (90.08%) when the RF signal is sent through the ports 1, 2, 3 and 4 respectively. The radiation pattern for the smart antenna that implements the ULA with metamaterial structures etched in the ground plane was also investigated. Figures 8 show the theoretical and simulated results. The summary results in both cases are shown in Tables VIII and IX. The results show that the antenna with metamaterial etched in the ground plane has a larger HPBW than a conventional ULA, which can improve in communication with nodes. The radiation efficiency was also evaluated in this case, and it achieves radiation efficiencies of -0.57 dB (87.7%), -0.8812 dB (81.63%), -0.8704 dB (81.83%), and -0.5765 dB (87.56%) when the RF signal enters through ports 1, 2, 3, and 4. According to the findings, the suggested fixed forming system may transfer radiation in at least four directions. Similarly, a good correlation was found between theoretical and experimental data, particularly when studying the conventional ULA's system.

TABLE VII
SIMULATED RADIATION PATTERN OF CONVENTIONAL ULA

Parameter/Input	Port 1	Port 2	Port 3	Port 4
Gain (dbi)	-35.09	-26.41	-28.38	-35.6
Main lobe direction (deg)	14	-39°	39	-13
HPBW (deg)	23.5	26	26.2	23.6

TABLE VIII
EXPERIMENTAL RADIATION PATTERN OF ULA
WITH METAMATERIAL ARRAY ETCHED IN GROUND PLANE

Parameter/Input	Port 1	Port 2	Port 3	Port 4
Gain (dbi)	-38.8	-26.3	-24.9	-29.8
Main lobe direction (deg)	15	-40	45	-5
HPBW (deg)	45	60	30	35

TABLE IX
SIMULATED RADIATION PATTERN OF ULA
WITH METAMATERIAL ARRAY ETCHED IN GROUND PLANE

Parameter/Input	Port 1	Port 2	Port 3	Port 4
Gain (dbi)	-33.29	-29.54	-29.9	-30
Main lobe direction (deg)	13	-39	37	-14
HPBW (deg)	24.1	27.1	26.5	24

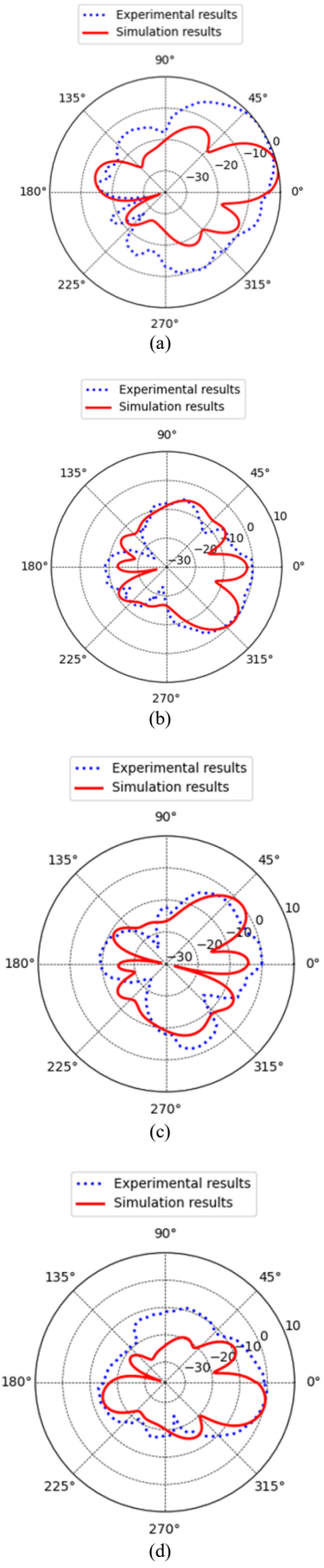

Figs. 8. Comparison between simulated and experimental radiation patterns of the beamforming system based on ULA loaded with metamaterial structures when the RF signal input trough (a) port 1 (b) port 2 (c) port 3 (d) port 4

Minor differences in the system that employs the ULA with metamaterial arrangement etched in the ground plane are the result of machine faults during device manufacturing and misalignment in the rotating base used to monitor the experimental radiation patterns. The radiation pattern in both circumstances, however, has the same shape and primary lobe orientations.

IV. Conclusion

In this work, a Butler matrix was designed, and evaluated. Then, the ability to this RF circuit to control the phase difference between the four output ports was demonstrated, which could be managed trough phase shifters, couplers, and crossovers. On the other hand, the Butler matrix was integrated with two different antenna arrays. Therefore, a fixed beamforming capable of transmitting data in at least four different directions while maintaining excellent electrical efficiency and operating at 2.4 GHz was developed. In addition, two unique smart antenna systems were created and tested experimentally.

The results reveal that the smart antenna based on conventional ULA gives a large gain in comparison with the ULA loaded with metamaterials etched in the ground plane. However, the alternative employing metamaterials provides a high HPBW in all circumstances, which can be helpful for connecting with receiving nodes.

Moreover, the performance of these smart antennas may be confirmed in both theoretical and experimental settings. When the RF signal is fed by ports 1, 2, 3, and 4, the system based on conventional ULA generates radiation at 30°, -35°, 49°, and -60°, respectively. When the test was performed using the ULA loaded with metamaterial arrays, comparable results were achieved.

Moreover, the complete system displays a high radiation efficiency, which corroborate the good impedance mismatch between all parts. Based on the findings, it was feasible to deduce that metamaterial structures can be used to improve the electrical performance of a beamforming system. Finally, the results of this research show that using metamaterial cells to improve fixed bemforming systems is possible. In fact, it is proposed in a future work to employ the technology presented in this paper as a wireless energy transmitter, with the aim of powering a network of wireless sensors distributed over four separate locations. Allowing to solve the present challenges with IoT devices that are used outside and consequently require sophisticated power supply systems such as solar panels or similar technologies.

Acknowledgements

The authors would like to express their gratitude to the Instituto Tecnologico Metropolitano, project P21101.

The author, S. Montoya-Villada, gratefully thanks the assistance of the Ministerio de Ciencia, Tecnologia, y Innovacion (Minciencias) through the program “Convocatoria fortalecimiento de vocaciones y

formación en CTeI para la reactivación económica en el marco de la postpandemia 2020".

References

[1] J. Botero Valencia, L. Castaño Londoño, and D. Marquez Viloria, Trends in the Internet of Things, *TecnoLógicas*, vol. 22, no. 44, pp. I–II, 2019.
doi: 10.22430/22565337.1241

[2] B. Huertas-Herrera, D. Góez Sánchez, and E. ReyesVera, Spectral Power Map Generation Based on Spectrum Scanning in the ISM Band for Interference Effects, in *Communications in Computer and Information Science*, 2020, vol. 1154 CCIS, pp. 3–15.
doi: 10.1007/978-3-030-46785-2_1

[3] E. Reyes-Vera, D. E. Senior, J. M. Luna-Rivera, and F. E. López-Giraldo, Advances in electromagnetic applications and communications, *TecnoLógicas*, vol. 21, no. 43, pp. 9–13, 2018.
doi: 10.22430/22565337.1052

[4] Guerra-Londono, M., Urrea, G., Botero-Valencia, J., Reyes-Vera, E. (2022). Design, Implementation, and Modeling of a LoRa Network Installed in a Freshwater Body. In: Narváez, F.R., Proaño, J., Morillo, P., Vallejo, D., González Montoya, D., Díaz, G.M. (eds) *Smart Technologies, Systems and Applications. SmartTech-IC 2021. Communications in Computer and Information Science*, vol 1532. Springer, Cham.
doi: https://doi.org/10.1007/978-3-030-99170-8_2

[5] M. Chryssomallis, Smart antennas, *IEEE Antennas Propag Mag*, vol. 42, no. 3, pp. 129–136, 2000.
doi: 10.1109/74.848965

[6] S. S. Jeng, G. T. Okamoto, G. Xu, H. P. Lin, and W. J. Vogel, Experimental evaluation of smart antenna system performance for wireless communications, *IEEE Trans Antennas Propag*, vol. 46, no. 6, pp. 749–757, 1998.
doi: 10.1109/8.686758

[7] G. H. Elzwawi, H. H. Elzwawi, M. M. Tahseen, and T. A. Denidni, requency selective surface-based switched-beamforming antenna, *IEEE Access*, vol. 6, pp. 48042–48050, Jul. 2018.
doi: 10.1109/ACCESS.2018.2850808

[8] H. J. Dong, Y. B. Kim, and H. L. Lee, Reconfigurable Quad-Polarization Switched Beamforming Antenna With Crossed Inverted-V Array and Dual-Butler Matrix, *IEEE Trans Antennas Propag*, vol. 70, no. 4, pp. 2708–2716, Apr. 2022.
doi: 10.1109/TAP.2021.3137258

[9] S. Kim, S. Yoon, Y. Lee, and H. Shin, A miniaturized butler matrix based switched beamforming antenna system in a two-layer hybrid stackup substrate for 5g applications, *Electronics (Switzerland)*, vol. 8, no. 11, Nov. 2019.
doi: 10.3390/electronics8111232

[10] M. Moubadir, A. McHbal, N. A. Touhami, and M. Aghoutane, A Switched Beamforming Network for 5G Modern Wireless Communications Applications., in *Procedia Manufacturing*, 2019, vol. 32, pp. 753–761.
doi: 10.1016/j.promfg.2019.02.282

[11] O. Ben Smida, S. Zaidi, S. Affes, and S. Valaee, Robust distributed collaborative beamforming for wireless sensor networks with channel estimation impairments, *Sensors (Switzerland)*, vol. 19, no. 5, 2019.
doi: 10.3390/s19051061

[12] Y. Han, S. Jin, J. Zhang, J. Zhang, and K. K. Wong, DFT-Based Hybrid Beamforming Multiuser Systems: Rate Analysis and Beam Selection, *IEEE Journal on Selected Topics in Signal Processing*, vol. 12, no. 3, pp. 514–528, 2018.
doi: 10.1109/JSTSP.2018.2821104

[13] E. Bjornson, M. Bengtsson, and B. Ottersten, Optimal multiuser transmit beamforming: A difficult problem with a simple solution structure [Lecture Notes], *IEEE Signal Process Mag*, vol. 31, no. 4, pp. 142–148, 2014.
doi: 10.1109/MSP.2014.2312183

[14] K. Haneda, E. Kahra, S. Wyne, C. Icheln, and P. Vainikainen, Measurement of loop-back interference channels for outdoor-to-indoor full-duplex radio relays, in *EuCAP 2010 - The 4th European Conference on Antennas and Propagation*, 2010.

[15] L. Rao, M. Pant, L. Malviya, A. Parmar, and S. V. Charhate, 5G beamforming techniques for the coverage of intended directions in modern wireless communication: In-depth review, *International Journal of Microwave and Wireless Technologies*, vol. 13, no. 10. Cambridge University Press, pp. 1039–1062, Dec. 15, 2021.
doi: 10.1017/S1759078720001622

[16] A. Shastrakar, Design and Simulation of Microstrip Butler Matrix Elements Operat-ing at 2.4GHz for Wireless Applications, *Int J Sci Eng Res*, vol. 7, no. 5, pp. 1528–1531, 2016.

[17] J. A. Cabrera Botero and C. I. Paez Rueda, Switched pattern antenna for the ISM band (2.45 GHz), *Ingenieria y Universidad*, vol. 18, no. 1, pp. 1–12, 2014.
doi: 10.11144/javeriana.iyu18-1.apca

[18] A. T. Devapriya and S. Robinson, Investigation on metamaterial antenna for terahertz applications, *Journal of Microwaves, Optoelectronics and Electromagnetic Applications*, vol. 18, no. 3, pp. 377–389, 2019.
doi: 10.1590/2179-10742019v18i31577

[19] L. M. Castellanos, F. Lopez, and E. Reyes - Vera, Metamateriales: principales características y aplicaciones, *Rev Acad Colomb Cienc Exactas Fis Nat*, vol. 40, no. 156, p. 395, 2016.
doi: 10.18257/raccefyn.345

[20] D. Catano-Ochoa, D. E. Senior, F. Lopez, and E. Reyes-Vera, Performance analysis of a microstrip patch antenna loaded with an array of metamaterial resonators, *2016 IEEE Antennas and Propagation Society International Symposium, APSURSI 2016 - Proceedings*, pp. 281–282, 2016.
doi: 10.1109/APS.2016.7695849

[21] F. Umaña-Idarraga, D. Cataño-Ochoa, S. Montoya-Villada, C. Valencia-Balvin, and E. Reyes-Vera, Design of a perfect and multi-resonant metamaterial absorber for electromagnetic energy harvesting applications, in *Journal of Physics: Conference Series*, Nov. 2021, vol. 2118, no. 1.
doi: 10.1088/1742-6596/2118/1/012005

[22] B. A. F. Esmail, S. Koziel, L. Golunski, H. B. A. Majid, and R. K. Barik, Overview of Metamaterials-Integrated Antennas for Beam Manipulation Applications: The Two Decades of Progress, *IEEE Access*, vol. 10, pp. 67096–67116, 2022.
doi: 10.1109/ACCESS.2022.3185260

[23] D. Shan, H. Wang, K. Cao, and J. Zhang, Wireless power transfer system with enhanced efficiency by using frequency reconfigurable metamaterial, *Sci Rep*, vol. 12, no. 1, p. 331, Jan. 2022.
doi: 10.1038/s41598-021-03570-8

[24] B. A. F. Esmail et al., Deflected beam pattern through reconfigurable metamaterial structure at 3.5 GHz for 5G applications, *Waves in Random and Complex Media*, pp. 1–24, Mar. 2022.
doi: 10.1080/17455030.2022.2053608

[25] A. Dadgarpour, B. Zarghooni, B. S. Virdee, and T. A. Denidni, Beam Tilting Antenna Using Integrated Metamaterial Loading, *IEEE Trans Antennas Propag*, vol. 62, no. 5, pp. 2874–2879, May 2014.
doi: 10.1109/TAP.2014.2308516

[26] B. A. F. Esmail, H. B. Majid, S. H. Dahlan, Z. Z. Abidin, M. K. A. Rahim, and M. Jusoh, Planar antenna beam deflection using low-loss metamaterial for future 5G applications, *International Journal of RF and Microwave Computer-Aided Engineering*, vol. 29, no. 10, Oct. 2019.
doi: 10.1002/mmce.21867

[27] A. Dadgarpour, A. A. Kishk, and T. A. Denidni, Dual band high-gain antenna with beam switching capability, *IET Microwaves, Antennas & Propagation*, vol. 11, no. 15, pp. 2155–2161, Dec. 2017.
doi: 10.1049/iet-map.2017.0294.

[28] L. Josefsson and P. Persson, *Conformal Array Antenna Theory and Design*. John Wiley and Sons, 2006.
doi: 10.1002/047178012X

[29] Ostankov, A., Shchetinin, N., Chernoyarov, O., Pergamenchtchikov, S., Broadband Beam-Forming Circuit Using Microstrip Multilayer Couplers, (2020) *International Journal on Communications Antenna and Propagation (IRECAP)*, 10 (5), pp. 295-301.
doi:https://doi.org/10.15866/irecap.v10i5.19371

[30] Shaji B. K., A., Pradeep, A., Mohanan, P., Fractal Inspired Metamaterial Superstrate for Gain Enhancement, (2021) *International Journal on Communications Antenna and Propagation (IRECAP)*, 11 (4), pp. 271-278. doi:https://doi.org/10.15866/irecap.v11i4.20861

[31] Thankachan, S., Paul, B., Electrically Small Metamaterial Inspired Monopole Antenna Using Double Negative Metamaterial and Ring Resonators, (2021) *International Journal on Communications Antenna and Propagation (IRECAP)*, 11 (6), pp. 440-448. doi:https://doi.org/10.15866/irecap.v11i6.21233

[32] Saleh, G., Dual Resonant Wearable Metamaterial for Medical Applications, (2021) *International Journal on Communications Antenna and Propagation (IRECAP)*, 11 (2), pp. 85-93. doi:https://doi.org/10.15866/irecap.v11i2.19856

[33] Raghavendra, C., Neelaveni Ammal, M., Madhav, B., Metamaterial Based Circularly Polarized Parasitic Element Driven DRA for Sub 6 GHz Wireless and 5G Communication Applications, (2022) *International Journal on Communications Antenna and Propagation (IRECAP)*, 12 (4), pp. 293-301. doi:https://doi.org/10.15866/irecap.v12i4.21228

Authors' information

[1]Department of Electronics and Telecommunications Engineering, Instituto Tecnológico Metropolitano, Medellín 050013, Colombia.

[2]Department of Mechatronics and Electromechanics, Instituto Tecnológico Metropolitano ITM, Medellín 050013, Colombia.

Sebastian Montoya-Villada was born in Itagüí, Colombia. He graduated from the Instituto Tecnologico Metropolitano in Medellin in 2021 as a telecommunications engineer. Microwave devices, Smart antennas, microstrip sensors, material substrate design, internet of things, and optical fiber sensors are among his research interests.

Juan Morales-Guerra was born in Bogotá, Colombia, and graduated from the Instituto Tecnológico Metropolitano, ITM (Medellin, Colombia) with a degree in telecommunications technology. He is now pursuing a telecommunications engineer degree, and his current research interests include antenna design and development, smart antennas, and artificial intelligence. In addition, he does research on communication and automation systems.

Daniel Catano-Ochoa was born in Girardota, Colombia. He received the B.S. degree in Telecommunications engineering from the Instituto Tecnológico Metropolitano, ITM (Medellin, Colombia) in 2018. He is pursuing a master's degree in automation and industrial control at Instituto Tecnológico Metropolitano since 2021.Finally, his current research interests include antenna design and development, smart antennas, and microwave devices.

Juan Zapata-Londono was born in Medellín, Colombia, on January 22,1999. Graduate on telecommunications technology in the Institute Metropolitan of Medellin, in 2020. He is currently pursuing the Telecommunications engineer and his current research interests include microwave sensors, antennas, and material characterization at microwave frequencies.

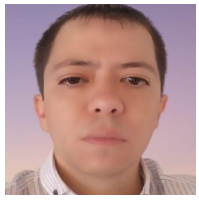

J. S. Botero-Valencia Magister in Automation and Industrial Control, and PhD in Engineering, has experience in control systems and robotics, specifically on the Internet of Things (IoT) and mobile robotics. He currently works as a Professor in the Department of Mechatronics and Electromechanics of the Faculty of Engineering of the Metropolitan Technological Institute and belongs to the Laboratory of Control Systems and Robotics.

Erick Reyes-Vera was born in Cúcuta, Colombia, in 1986. He received the B.S. degree in physics engineering and the M.S. degree in physics from the Universidad Nacional de Colombia, Medellin, in 2009 and 2014, respectively. He also received the Ph.D. degree in electrical engineering from the Universidad Nacional de Colombia, Bogota, in 2020. In 2013, he joined the Department of Electronics and Telecommunications, Instituto Tecnológico Metropolitano, ITM (Medellin, Colombia). His research interests include optical fiber sensors, photonic crystal fibers, photonic devices, planar antennas, microwave devices, microwave sensors, and the characterization of materials at microwave frequencies. He has published 39 articles, 2 book chapter, one patent, and 20 conference papers in these research areas. Dr. Reyes-Vera has served as a reviewer for several journals, including Applied Optics, Optic Express, Optics Letters, International Journal on Communications Antenna and Propagation, IEEE Sensors Journal, IEEE Sensors Letters, Sensors and Actuators, Progress in Electromagnetics Research, Optical Engineering, and Optical and Quantum Electronics.

